# Adsorption-Induced Kondo Effect in Metal-Free Phthalocyanine on Ag(111)

Julien Granet, Muriel Sicot, Iann C Gerber, Geoffroy Kremer, Thomas Pierron, Bertrand Kierren, Luc Moreau, Yannick Fagot-Revurat, Simon Lamare, Frédéric Cherioux, et al.

# Adsorption-Induced Kondo Effect in Metal-Free Phthalocyanine on Ag(111)

J. Granet,[†] M. Sicot,[*,†] I. C. Gerber,[‡] G. Kremer,[†,¶] T. Pierron,[†] B. Kierren,[†] L. Moreau,[†] Y. Fagot-Revurat,[†] S. Lamare,[§] F. Chérioux,[§] and D. Malterre[†]

†*Université de Lorraine, CNRS, IJL, F-54000 Nancy, France*

‡*Université de Toulouse, INSA-CNRS-UPS, LPCNO, 135 Avenue de Rangueil, 31077 Toulouse, France*

¶*Département de Physique and Fribourg Center for Nanomaterials, Université de Fribourg, CH-1700 Fribourg, Switzerland*

§*Univ. Bourgogne Franche-Comté, FEMTO-ST, CNRS, UFC, 15B avenue des Montboucons, F-25030 Besançon cedex, France*

## ABSTRACT

We report on the formation of a two-dimensional supramolecular Kondo lattice made of organic molecules comprising only C, N and H atoms namely metal-free phthalocyanines 2HPc ($C_{32}H_{18}N_8$) adsorbed on a Ag(111) surface. Low-temperature scanning tunneling microscopy/spectroscopy (LT-STM/STS), ultra-violet photoemission spectroscopy (UPS) and density functional theory (DFT) are used to investigate the electronic structure of the system for low molecular density and commensurate self-assemblies. Abrikosov-Suhl resonances that are characteristic of the arising of a Kondo effect are observed using both STS and UPS at low temperature. Whereas freestanding 2HPc is a no-spin bearing molecule, it acquires an unpaired electron in its $\pi$-conjugated lowest unoccupied molecular orbital (LUMO) upon adsorption on Ag. As a result, the Kondo effect can

be interpreted as originating from the interaction between this unpaired $\pi$-spin and the Ag Fermi sea. Extra side resonances are observed in STS spectra that are a manifestation of the coupling between the $\pi$ electron and molecular vibrational excitations, qualifying the effect as molecular vibrational Kondo effect. The variation of the Kondo temperature $T_K$ of single molecules and upon two-dimensional self-assembly is discussed. This study brings new insights in the Kondo-related physics in correlation with molecular spins and low-dimensionality. Moreover, it may open new routes to the synthesis of organic molecular spintronic devices.

# INTRODUCTION

Molecular magnetism have attracted rising attention since molecular based magnetic materials can have many technological applications in areas such as quantum computation,[1,2] high-density data storage and spintronics.[3–7] Very early in the development of the field, metallophthalocyanines (MPc) have proven to be a priviledged class of molecules to study magnetism at the nanometer scale.[8–11] Indeed, many MPc possess unpaired electrons in the gas phase and thus have non-zero magnetic moments. Besides, bis-phthalocyanines sandwiching rare-earth ions have been shown to behave as single-molecular magnets.[12,13] Their applicative potential has already been demonstrated, for example by fabricating functional supramolecular spin valves.[14]

The attractiveness of these molecules also lies in their easy synthesis, low cost and industrial avaibility. Particularly, they can be evaporated under ultra-high vacuum (UHV) allowing the synthesis of thin films.[15] In addition, the planar geometry of their $\pi$-conjugated ligand that can lie parallel to the surface on which they are adsorbed is an asset: the flatness of MPcs allows direct hybridization with the orbitals of the underlying substrate leading to the modification of surface properties and new exotic phenomena when in contact with various substrates such as ferromagnetic (FM) materials,[4] topological insulators, supraconductors or 2D materials.[16–18] For instance, in the case of the MPc/FM molecular spinterfaces, it has been shown that the addition of MPc increases or invert the FM spin-polarization which is a key property regarding performance of spin devices.[19–22] In the case of CoPc/$Bi_2Se_3$, Caputo;et al. have evidenced by angular-resolved photoelectron spectroscopy (ARPES), the modification of the topological surface states and the energy shift of the Dirac cone due to charge transfer from the molecule to the surface[23]. When in contact with superconductors, magnetic nano-objects can be envisaged as qubits for quantum computing devices. In such cases, the governing factor is the strength of spin-superconductor interactions. MPc/Pb(111) interfaces have been shown to be ideal platforms to tune locally this magnetic interaction strength by adsorbing the molecules on different sites or by continuously varying it using the interaction with an STM tip.[24,25] Finally, optical measurements of MPc/$MoS_2$ heterojunctions evidenced charge transfer that is sensitive to the transition metal core. This property allows for

tuneable optical absorption making those systems interesting for optoelectronic applications.[16]

Moreover, this flat-lying molecular adsorption configuration offers an open area to the vacuum side. This gives the opportunity to manipulate the spin-state using on-top adsorption of alkali atoms or molecules to induce electron doping. Such studies have led to the emerging research field of on surface-magnetochemistry.[26,27]

In many cases, interfacial properties result from the hybridization of the highly directional $d_{z^2}$-orbital of the core metal atom with those of the substrate. Yet, for other MPc/inorganic interfaces, coupling can arise from hybridization with the $\pi$ ($p_z$) orbital of the Pc ligand, as well. The filling of the $\pi$-orbital by charge transfer modifies the spin state of the molecule in comparison with the free one. As an example, it was shown that the no-spin bearing NiPc molecule acquires a $1/2$-spin of $\pi$-origin due to charge transfer upon adsorption on a Ag(100) single-crystalline surface.[28,29] This has been demonstrated by revealing the spectral signature which is typical of a $1/2$-spin object in interaction with an electron bath namely an Abrikosov-Suhl resonance of the differential conductance in the vicinity of the Fermi level $E_F$ using LT-STM/STS resulting from Kondo effect.[30–35] On the same Ag(100) surface, CuPc which possesses a $1/2$-spin state in its ground state, acquires an extra $\pi$-electron. In this last case, the molecule behaves as a two-spin system in contact with conduction electrons leading to an interesting many-body phenomenon: a triplet-singlet Kondo effect.[28] Alternatively, STM and UPS measurements recorded on the CoPc/Ag(111) interface have unravelled another more complex donation/backdonation scenario: electron injection occurs from the Ag substrate to the Co-$3d$ orbitals that is accompagnied with a back donation of electrons from the $\pi$-orbitals to the substrate.[36]

Recently, it was shown by UPS that the metal-free phthalocyanine 2HPc which is a no-spin bearing molecule in the gas phase can also become charged upon adsorption on Ag(111).[37–39] We can therefore wonder if this system could also exhibit a Kondo effect as in the case of NiPc or CuPc on Ag(100). The implication of such a result would be that a purely organic phthalocyanine adsorbed on a silver surface could give rise to interesting magnetic properties without the involvement of $3d$ transition metal nor $4f$ rare-earth central ions as in previous studies. Indeed, only very

few examples of pure organic systems presenting Kondo effect have been reported so far.[40–45]

Despite the increasing attention devoted to the abovementioned hybrid MPc/inorganic interfaces, however the spin-polarized electronic properties of the 2HPc/Ag(111) interface had been underlooked.[37–39,46] Yet, this particular system could provide a means of investigating many-body phenomena such as Kondo effect in many aspects,*e.g.* its intensity, spatial extension,[47] quantum criticality[44] when a $^1/_2$ spin in $\pi$ orbital is involved rather than a $3d$ or $4f$-orbital. It would therefore broaden our knowledge on magnetism as well as on many-body physics at the nanometer scale and at low dimensionality.[40–43,47–62] Moreover, as illustrated above, a full description of the hybrid interfaces must necessarily consider both interfacial sides. On the metal side, sizeable modifications can also be expected as already observed with other $\pi$-conjugated molecules at the interface with copper or silver surfaces.[39,63–67] In the case of 2HPc/Ag(111), it has been shown that upon molecular adsorption, an interfacial state forms originating from the well-known bare metal Shockley state.[39,68,69] Those hybrid interfacial states (HIS) are of particular importance for the understanding of contact in organic semiconductor devices and their origin are not yet fully understood[63,67]. Therefore, such a study might also unravel insights on the Ag hybrid interface state.

In this framework, we have investigated by LT-STM/STS, UPS and DFT, the electronic structure of adsorbed 2HPc on Ag(111) for single molecules as well as for two-dimensional self-assembled molecular networks. We demonstrate the emergence of a Kondo effect regardless of the coverage in the submonolayer regime. We think that this kind of hybrid interface with molecules comprising only C, H and N-atoms may thus be envisaged to design metamaterials composed of abundant and environmental-friendly compounds.

# METHODS

The experiments were carried out in two ultra-high vacuum systems with a base pressure of $1 \times 10^{-10}$ mbar. One was equipped with a low-temperature Omicron STM operating at $5\,\mathrm{K}$. The other one was equipped with a ScientaOmicron DA30-L hemispherical analyzer and a monochromatized

$He_I$ ($h\nu = 21.2$ eV) UV source for ARPES. As beam damage of the molecular layers was observed on a timescale of about $20$ min, duration of the measurements and sample position were adjusted accordingly. Due to angular distribution of the photoemission intensity, ultra-violet photoemission spectra were recorded at an emission angle of $45°$.[54,70,71] Note that, in this geometry, the Shockley surface state of Ag(111) lying in the L-gap around the $\Gamma$ point of the surface Brillouin zone is not detected[69]. All spectra were normalized to the count rate at the binding energy of $0.4$ eV. LEED was available on both UHV set-ups to characterize structural properties at a sample temperature of $80$ K. The Ag(111) single crystal was cleaned by repeated cycles of $Ar^+$ sputtering at an energy of $1$ keV followed by an annealing to $800$ K. 2HPc molecules were purchased from Aldrich and purified by column chromatography (silica gel, dichloromethane) prior to use. They were evaporated from a Knudsen cell at $565$ K onto the sample held at room temperature. The STM images were recorded at a tunneling current $I_t$ and a bias voltage $V_b$ where the sign corresponds to the voltage applied to the sample. STS was acquired with a PtIr scissors-cut tip and a lock-in detection in open feedback loop conditions at a frequency of $1100$ Hz and a peak-to-peak bias voltage modulation for high-resolution STS of $5$ mV.

The electronic structures were obtained from DFT calculations with the VASP package[72–75] which uses the plane-augmented wave scheme[76,77] to treat core electrons. Perdew-Burke-Ernzerhof (PBE) functional[78] was used as an approximation of the exchange-correlation electronic term, but PBE-D3 scheme[79,80] was used firstly to optimize the geometry since Huang;et al. have addressed the importance of van der Waals corrections when dealing with Pc-metallic surfaces interactions.[81] The kinetic energy cutoff was set to $400$ eV, with a gaussian smearing of $0.05$ eV and using a $2\times2\times1$ k-points grid to optimize the structures with a convergence force criterium of $0.01$ eV/Å for all allowed atoms to relax. For density of states (DOS) determinations, a $3\times3\times1$ k-points grid was used in conjunction with the tetrahedron method with Blöchl corrections scheme.[82] We have confirmed that a 12 layers-slab with a vacuum height of more than $20$ Å was necessary to describe accurately the intrinsic Shockley surface state of the Ag (111) surface,[83] see Fig. S3 for a band structure representation in the Supporting Information. As expected, two surface states

are provided by the slab approach and the average energy of the two surface states ($-86$ meV) is relatively close to the experimental energy value ($-63$ meV).[69] To mimic the individual molecule case, as well as to describe the C-phase, see definition below, a ($7\times7$) and commensurate ([5 0; 3 6]) cell was used respectively.

# RESULTS AND DISCUSSION

## Structural Properties

The growth of 2HPc on Ag(111) in the submonolayer regime has been studied in previous works. Three distinct phases form as a function of the coverage.[38] For self-assemblies, the unit cells have been determined.[38] Yet, the adsorption geometry and especially the azimuthal orientation of the molecules has only succinctly been addressed and remains elusive, particularly in self-assemblies. Nevertheless, this information is of paramount importance to elucidate the electronic properties of the metal-organic interface. Thanks to STM images with intramolecular resolution, we were able to tackle this key point as will be explained below.

According to Kröger;et al., at low molecular densities, 2HPc form disordered gas-like phases, referred as G-phases where the intermolecular distance changes with coverage due to substrate-mediated intermolecular repulsive interaction.[38] Upon increasing coverages to 0.5-0.89 monolayers at low temperature, they form a commensurate phase with the substrate referred as C-phase, characterized by a nearly-square unit cell which epitaxy matrix is [5 0;3 6].[38] Our LEED patterns displayed in Fig.1(a) and Fig.2(a) exhibiting a diffuse ring around the [00] specular beam and sharp spots, respectively are in line with those previous results. Sperl;et al. showed that 2HPc adsorb flat onto the Ag(111) substrate *i.e.* the Pc ligand plane adsorbs parallell to the surface plane.[46] The line formed by the two pyrrolic hydrogen atoms inside the porphyrazine core which will be referred to "the 2H-axis" hereafter, was shown to be azimuthally oriented perpendicular to $\langle 01\bar{1}\rangle$ cristallographic directions of the substrate. This was later confirmed by Kügel *et al.*[84] In C-phase, Bai;et al. measured by STM an azimuthal angle between one vector of the unit cell and the molecular

axis of about $60^\circ \pm 3^\circ$ without specifying the orientation of the 2H-axis.[85] In the present work, we determine the orientation of single molecules by comparing their STM appearance in Fig.1(b) with the HOMO of the singly charged 2HPc anion calculated in ref.[86] for which the splitted lobes are perpendicular to the 2H-axis. The specific choice of comparison with the anion is justified by the fact that the molecule gets negatively charged when adsorbed as we will discuss below. The direction of the 2H-axis of the molecules is highlighted by blue lines in Fig.1(b). Our STM images reveal that 2HPc not only adsorb with 2H-axis perpendicular to $\langle 01\bar{1} \rangle$ directions (i.e. along $\langle 2\bar{1}\bar{1} \rangle$ directions) as observed in literature[46,84] but also parallell (within an angle error of $\pm 2^\circ$). Molecules marked as C and C' in Fig. 1(b) are representative of the two configurations. Likewise in Fig. 1(c), molecules A and B adsorb in the same configuration as molecule C. In their recent work, Kügel and coworkers demonstrate that the only way to obtain a 2H-axis along one of the $\langle 01\bar{1} \rangle$ direction is to start with a molecule which 2H-axis is perpendicular to one $\langle 01\bar{1} \rangle$ direction and induce tautomerization by applying a bias voltage pulse U such that $|U| > 0.45$ V when the tip is located above the molecule. It is claimed that the absence of 2H-axis along $\langle 01\bar{1} \rangle$ directions can be explained by a high difference in energy with the configuration where the 2H-axis lies perpendicular to $\langle 01\bar{1} \rangle$.

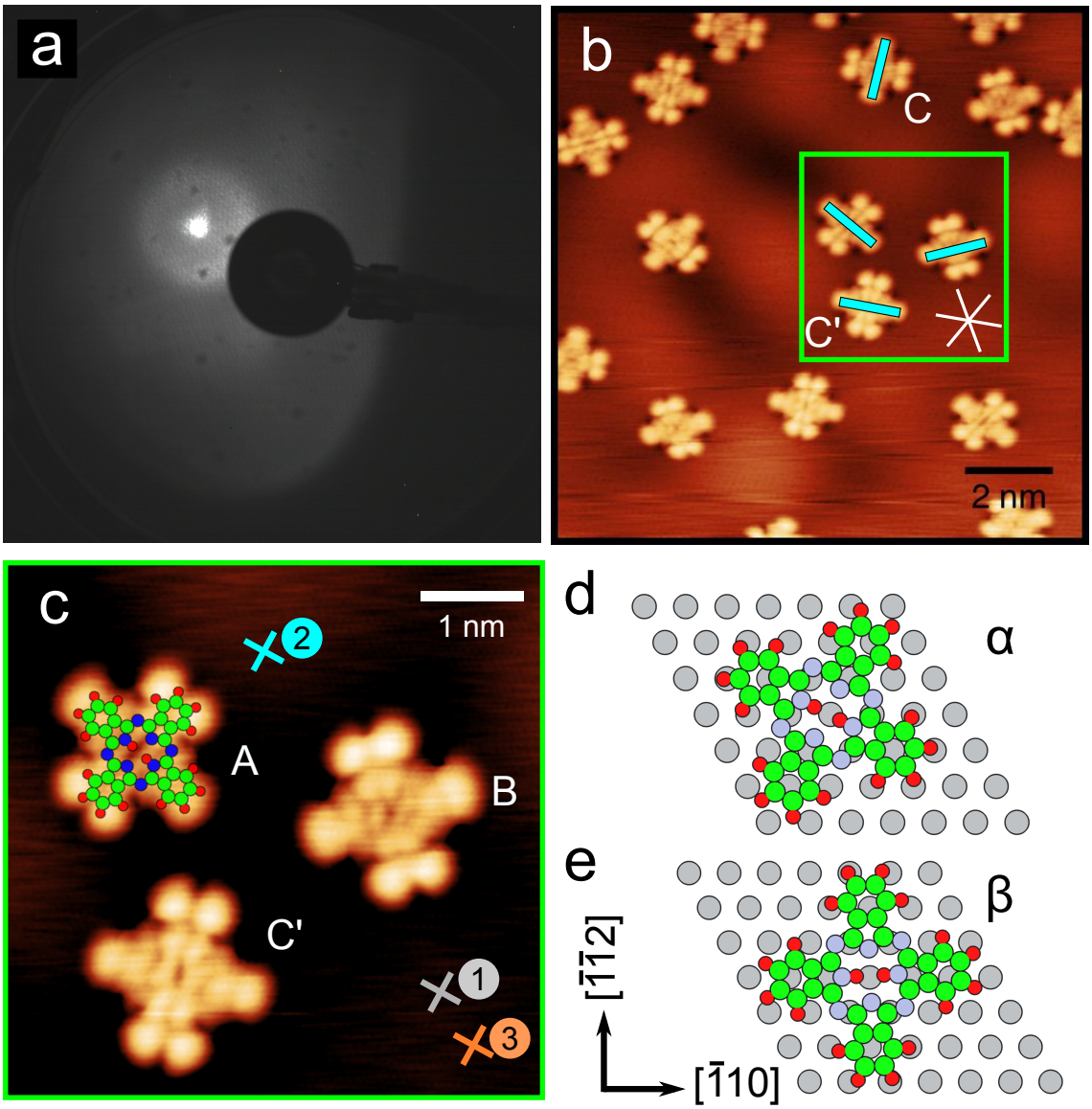


Figure 1: The Structure of 2HPc/Ag(111) in G-phase. (a) LEED pattern recorded at an electron energy of 15 eV. (b,c) High-resolution STM topographic images of 2HPc molecules on Ag(111). Tunneling bias conditions: $V_b = 1$ mV, $I_t = 200$ pA. The close-packed $\langle 01\bar{1} \rangle$ directions of the Ag(111) are indicated by white lines in (b). The numbered crosses in (c) indicates the location where the STS spectra displayed in Fig.3(a) and Fig.5(a) were recorded. Cyan lines in (b) indicate the direction of the 2H-axis (see text) of the molecules. (d,e) Top views of the DFT calculated relaxed most stable adsorption geometries.

On the contrary, in our work, we find two adsorption orientations that can simply be explained by molecules that could rotate in the ligand plane. Fig.1(d,e) displays the two simulated most stable adsorption configurations $\alpha$ and $\beta$ corresponding to 2H perpendicular and parallell to $\langle 01\bar{1} \rangle$ directions, respectively in good agreement with our observations. The difference of adsorption energy between these two geometries of minimum energy is only of about $0.2$ eV. Molecules A, B and C would therefore correspond to the $\alpha$-case (Fig.1(d)), whereas molecule C' would correspond to the $\beta$-case (Fig.1(e)). From these models, one can see that the transition from one geometry to the other can occur simply via a rotation of the molecule by $30^{\circ}$. In our work, we found compelling evidences that such rotation can happen. In Fig. S4 in the Supporting Information, two time sequences issued from pairs of STM images recorded successively show molecules that rotate without external stimuli other than the scanning tip governed by the tunneling parameters $V_b$, $I_t$ with $V_b$ much smaller than the bias voltage threshold necessary to induce tautomerization. For the particular coverage shown in Fig.1(b), the ratio of parallell to perpendicular configurations is 1/3 leading to the conclusion that the perpendicular geometry is the most stable one.

In the STM image of the C-phase displayed in Fig. 2(b), each molecule exhibits a pair of splitted lobes. Assuming that they are perpendicular to the 2H-axis as in the case of molecules in G-phase, the azimuthal angle $\delta$ with respect to the close-packed directions of Ag(111) as sketched in Fig. 2(b) can be determined. The measured value of $\delta$ is $65^{\circ} \pm 3^{\circ}$ similar within the angle error to the azimuthal orientation of the experimentally most stable adsorption configuration $\alpha$. The structural model of the molecules self-organized as a C-phase obtained by DFT calculations is shown in Fig.2(c). The angle $\delta = 62^{\circ}$ is in excellent agreement with the experimental value validitating this model to further extract the projected density of states (PDOS). The extra insight we get from this STM analysis is that molecules in the less stable configuration such as molecule C' in Fig.1 (b) undergo an azimuthal rotation of about $30^{\circ}$ upon self-assembling. Therefore, one expects the ratio between the two configurations to increase when increasing the coverage in favor of $\alpha$ configuration. However, this analysis is out of the range of this paper.

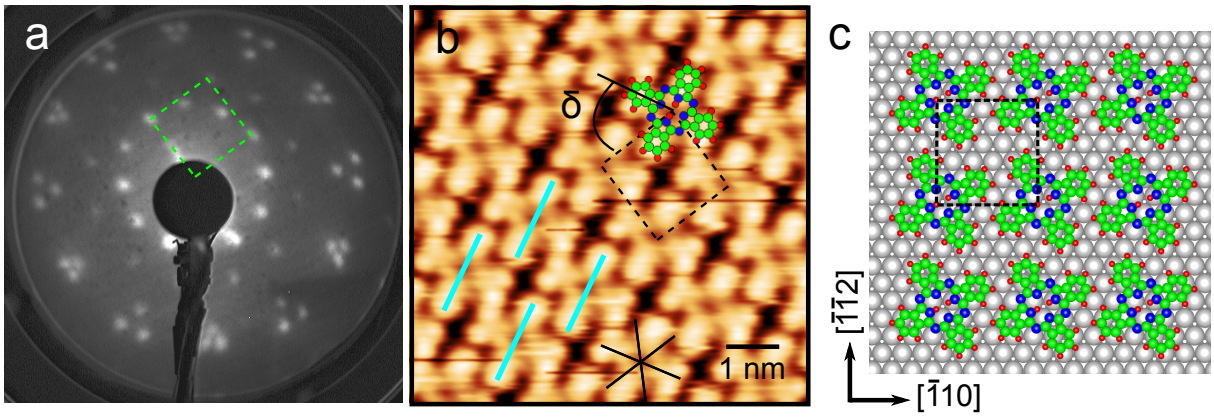


Figure 2: The Structure of 2HPc/Ag(111) in C-phase. (a) LEED pattern recorded at an electron energy of 14 eV. (b) Corresponding STM topographic image. Tunneling bias conditions: $V_b = -1.8$ V, $I_t = 200$ pA. The close-packed $\langle 01\bar{1} \rangle$ directions of the Ag(111) are indicated by a black star. Cyan lines indicate the direction of the 2H-axis of the molecules (see text). (c) Top view of the simulated relaxed adsorption geometry. Rectangles in dashed line represent the unit cells in (a) reciprocal and (b,c) direct space.

## Kondo effect in single molecules

In previous works, it was demonstrated from UPS and two-photon photoemission (TPPE) measurements that charge transfer occurs from the Ag(111) substrate to the Pc ligand of 2HPc.[38,39] In the C-phase, this was evidenced by the occupancy of the LUMO orbital upon adsorption resulting in a state located at an energy of $-0.15$ eV and which has been called former-LUMO (F-LUMO) in reference to the LUMO state of the free molecule. In addition, an unoccupied HIS develops from the former Shockley-type electronic state of the bare Ag(111) surface. It originates from the steepening of the surface potential upon molecular adsorption. This nearly-free electron state has been characterized by a band onset located at an energy of $+0.23 \pm 0.03$ eV above $E_F$.[39] Knowing the abovementioned results, one can reasonably raise the following question: would self-assembled 2HPc behave like 1/2-spin in contact with a free electron bath possibly giving rise to Kondo effect? Would this effect persists for single molecules? To elucidate the arising of a Kondo effect for

a single molecule as well as for a self-assembly, we performed STS and UPS on G and C-phases.

First, we address the Kondo effect in single molecules using STS and UPS. STS spectra in the enery range around $E_F$ are reported in Fig.3(a). They were recorded with the STM tip located above molecules A, B and C' displayed in Fig.1(c). All tunneling spectra show two main characteristics: (i) a sharp electronic resonance in the close vicinity of $E_F$ , labeled $\kappa$ in Fig.3(a), (ii) a conductance peak located at about $+52$ meV, labeled $\nu$. As no molecular nor substrate's state is expected in a range of $\pm 10$ meV around $E_F$, we can, as a first guess, reasonably attribute the resonance at $E_F$ to Kondo effect. Yet, as other phenomena could lead to the formation of a peak in the differential conductance spectrum next to $E_F$, a magnetic field or temperature dependency of the full width at half maximum (FWHM) of the resonance should be recorded and compared to laws governing the effect in order to unambiguously attribute its origin to Kondo effect.[87,88] Alternatively, UPS can be used since a typical spectrum of a Kondo system exhibits a sharp resonance at $E_F$ at temperatures below the Kondo temperature $T_K$ .[87,89,90] Upon increasing temperature, this peak is expected to broaden and decrease in intensity.[91–93] Such a relationship with temperature is what is experimentally observed as displayed in Fig. 3(b) showing UPS spectra recorded at temperatures of $9$ K, $80$ K and $285$ K. At T$= 9$ K, a narrow and intense peak is observed at $E_F$ . At T$= 80$ K, the peak is broader and its intensity is strongly reduced to finally almost vanish at T$= 285$ K.

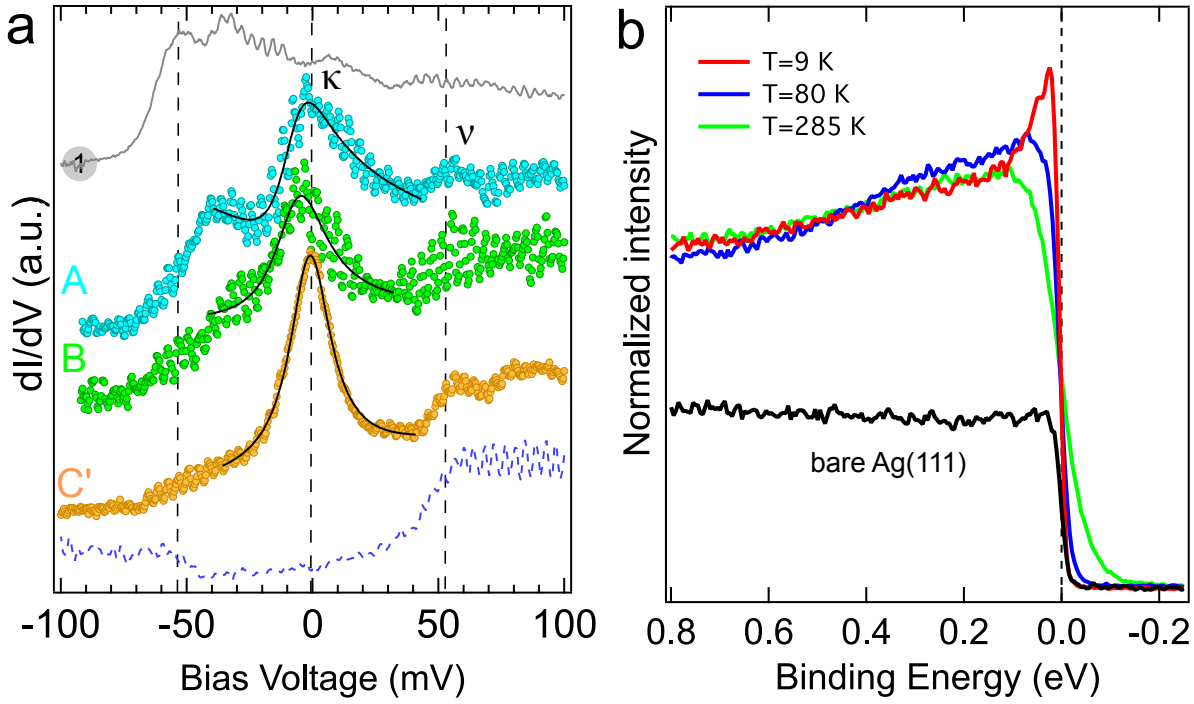


Figure 3: Electronic properties of 2HPc/Ag(111) in G-phase. (a) Dotted lines are dI/dV spectra recorded with the tip on top of molecules labeled A,B and C' in Fig.1(c). Set point is: $V_b = 1$ mV, $I_t = 200$ pA. The dashed blue line is a dI/dV spectrum recorded on a $4^{th}$ molecule (not in Fig.1(c)). Set point : $V_b = 25$ mV, $I_t = 200$ pA. The full grey line was recorded further away from the molecules on bare Ag surface at the position indicated by the grey cross in Fig. 1(c). The Fano fits represented by the black lines yields: A: $q = 1.73$, $\epsilon_K = -7.99$ meV and $\Gamma = 11.78$;B: $q = 7.22$, $\epsilon_K = -6.25$ meV and $\Gamma = 12.39$;C': $q = 54$, $\epsilon_K = -1.16$ meV and $\Gamma = 9.8$. A vertical shift was added for clarity. (b) UPS spectra recorded at T= 9 K, 80 K and 285 K and on bare Ag(111) substrate at T= 9 K (black line) and at an emission angle of $45°$.

The resonance observed in UPS spectra can not be assigned to any state of the substrate since the UPS spectrum recorded under the same experimental conditions on the bare Ag(111) surface is flat next to $E_F$ as shown as a black line in Fig.3(b). Thanks to the concomitance of a resonance at $E_F$ in the STS spectrum and the temperature behavior of the photoemission feature at $E_F$ , one can now unambiguously attribute it to a Kondo resonance.

The next feature of the STS spectra to be discussed is the peak $\nu$ at $E_\nu = 52 \pm 5$ meV. This side

feature appears as a resonance and its intensity with respect to the zero-bias one depends on the tip location. Upon certain tip conditions (see supplementary information for further details), the Kondo resonance is not observed. In those cases, the dI/dV spectrum has an upside down hat shape as depicted in Fig.3(a). The two step-edges are located at about $\pm E_\nu$ which is the standard lineshape observed when inelastic processes corresponding to vibrational excitation energies of $E_\nu$ get activated. However, the side feature appears more as a resonance than as a step. According to,[94–98] it can be understood as originating from the splitting of the zero-bias resonance resulting from the electron-vibron coupling. Other Kondo organic/inorganic systems exhibit as well, such peaks of vibronic nature.[28,29,40,99,100] In particular, conductance spectra recorded over CuPc and NiPc on Ag(100) exhibit such fingerprints at comparable excitation energies[28,29] and might correspond to the activation of torsion modes.[101]

According to Refs.,[32,33] $T_K$ can be roughly determined by fitting the Kondo resonance with a Fano function lineshape expressed as, disregarding the instrumental broadening:[102,103]

$$\frac{(q+\epsilon)^2}{(1+\epsilon^2)};\ \ \epsilon = \frac{eV-\epsilon_k}{\Gamma} \tag{1}$$

where $\Gamma$ is the 1/2 FWHM such that $\Gamma = k_B T_K$, $q$ the Fano asymmetry parameter and $\epsilon_k$ the energy shift of the resonance from $T_K$ .

As an example, the fitting results of the dI/dV spectra recorded at the center of molecules A, B and C' are reported in Fig. 3(a) as black lines. Another set of 4 measurements is shown in Fig.S1. The mean fitted $T_K$ is $T_K = 130\,\mathrm{K}$ with a standard deviation of $20\,\mathrm{K}$ and $q$ ranges from $0.3$ to more than $50$. The high q values indicates that the tunneling process occurs preferentially through the molecular orbital than to the conduction-electron continuum. Strong lineshape and FWHM variations are observed between the molecules. The possible influence of the adsorption configuration will be discussed below in relation to DFT calculations.

## Kondo effect in self-assembly

To investigate the arising of a Kondo effect in the commensurate self-assembly, STS and UPS were carried out. Results are displayed in Fig.4. To start with, STS was recorded over a large bias voltage range to investigate the overall electronic properties of the interface. Whereas UPS probe occupied states only, STS gives access to energy regions above and below Fermi level in a single-shot experiment enabling a direct comparison with UPS and TPPE spectra of previous studies.[38,39] The differential conductance dI/dV spectrum in Fig.4(a) reveals distinct peaks that can unambiguously be assigned. Peaks located at about $-0.12$ V and $-1.2$ V are attributed to F-LUMO and HOMO, respectively according to ref.[38,104] At positive bias, the step-like feature which is typical of a nearly-free electron two-dimensional gas is assigned to the HIS. Its edge is located at $+0.23 \pm 0.01$ V, in very good agreement with the band edge measured by TPPE.[39] The F-LUMO and HOMO states are also detected by UPS as indicated in Fig.S5 in the Supporting Information. As already explained in ref.,[38] the presence of an occupied F-LUMO state results from the charge transfer from the Ag surface to the molecule. Hence, both our STS and UPS experiments show that the molecule is negatively charged in agreement with these previous results. As well as for single molecules, a resonance at $E_F$ was obtained using STS and UPS techniques. Bringing forward the same arguments as for the case of single molecules, one can conclude that this resonance is the experimental signature of the Kondo effect. A high-resolution STS spectrum in Fig.4(b) exhibits, as in the case of single 2HPc, an extra peak at about $50$ meV leading to the conclusion that electron-vibron coupling is not hindered by intermolecular interactions inside the self-assembly thus resulting in a vibrational Kondo effect. Once again, this is corroborated by the inelastic electron tunneling spectrum shown in blue line in Fig.4(b) recorded over the Pc ligand and exhibiting the characteristic symmetric two-step like lineshape. The Kondo temperature $T_K$ obtained by fitting the STS spectra recorded over 7 molecules inside the supramolecular network ranges from $57$ to $69$ K as displayed in Fig. S2. It is about twice smaller than for single molecules. Possible explanations for the difference between the two phases will be discussed in section V.

## Density of states calculated by DFT

In order to correlate spectroscopic peaks observed in STS and UPS spectra with the molecular electronic structure, we have computed the DOS of 2HPc in C-phase and projected it onto atomic orbitals. As shown in Fig.4(d), this PDOS is dominated by $p_z$ orbitals. One peak below $-1$ eV corresponds to the HOMO state. Crossing $E_F$, another prominent peak of $p_z$ character corresponds to the F-LUMO state. Although the calculated energy position of this state is upshifted compared to experiments due to a well-known drawback of standard DFT calculations that do not properly account for HOMO-LUMO gap, it remains in good agreement with experimental data and supports the identification of the electronic states of the dI/dV spectrum of Fig.4(a).

A net charge transfer of $0.32e^-$ of $sp$-orbital character occurs from the substrate to the adsorbate region. Again, this value is only qualitative since charge transfer estimated from DFT calculations depends critically on the computational details.[105] Spin density distributions have been calculated as well and are shown in Fig.4(e). Obviously, the no spin bearing free 2HPc molecule does not exhibit any spin density (Fig.4(e),left). However, upon adsorption on Ag(111), (Fig.4(e),right) we observe a distribution of the spin electron density in the inner region of the molecule situated mostly on the pyrrole parts. This is very similar to what is observed for the anionic species as displayed in Fig.4(e) (center panel). The DFT results confirm the scenario that the origin of the Kondo effect lies in the filling of the molecular $\pi$ states occuring upon adsorption on the silver surface.

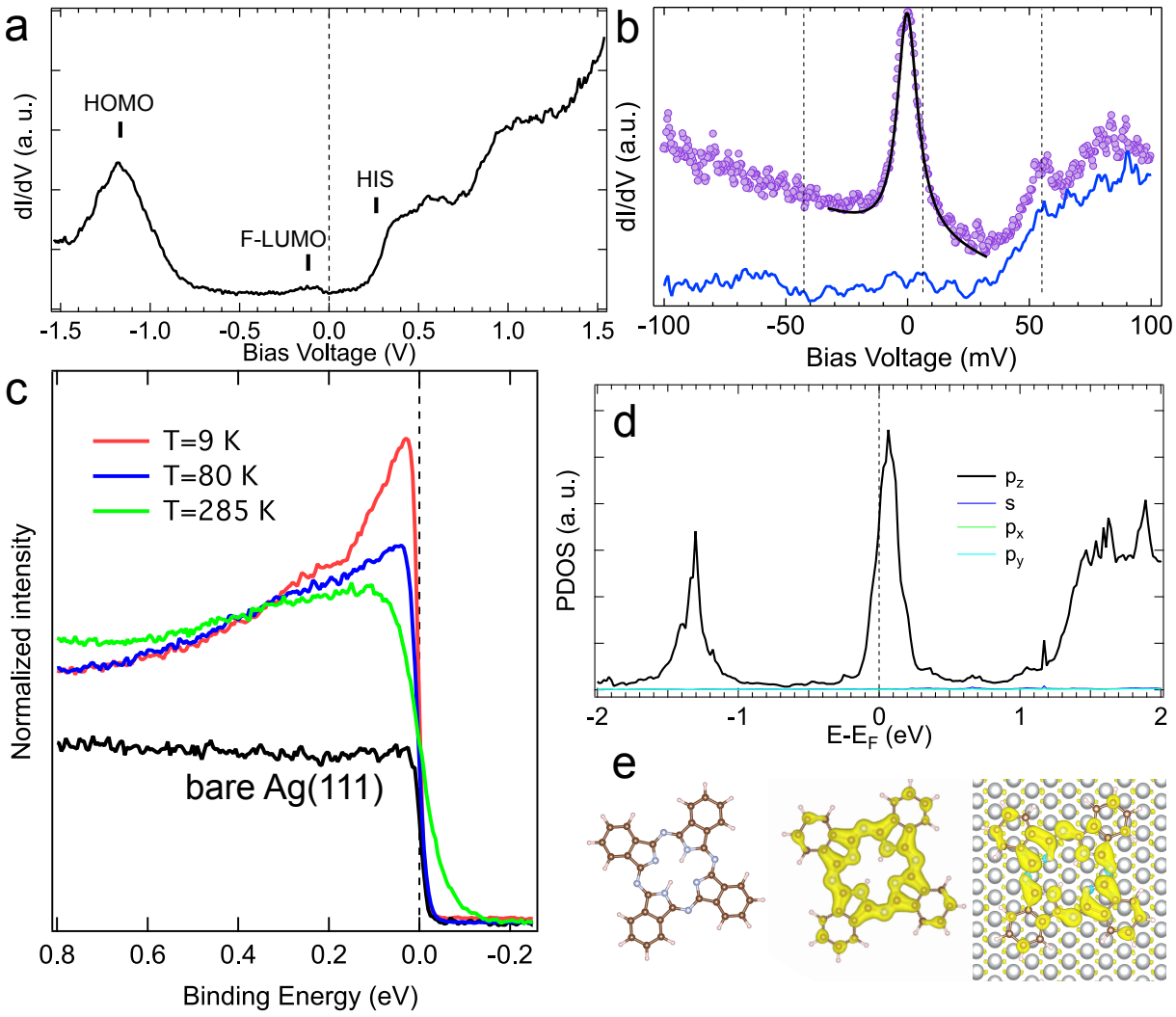


Figure 4: Electronic properties of 2HPc/Ag(111) in C-phase. (a,b) dI/dV spectra recorded over the center of one molecule in the self-assembly. Set point are (a) $V_b = -1$ V, $I_t = 100$ pA, (b) $V_b = 1$ mV, $I_t = 200$ pA for top curve and $V_b = 50$ mV, $I_t = 200$ pA for bottom curve. A vertical shift was added for clarity. The Fano fit represented by the black line superimposed to the top curve in (b) yields: $q = 21$, $\epsilon_K = -0.35$ meV and $\Gamma = 5.0$. (c) UPS spectra recorded at T= 9 K, 80 K, 285 K and on bare Ag(111) substrate at T= 9 K at an emission angle of $45°$. (d) Computed density of states projected (PDOS) onto atomic orbitals of 2HPc on Ag(111), (e) from left to right: spin density distribution of neutral, anionic 2HPc species in the gas-phase and adsorbed on Ag(111). The sign of the spin is indicated in yellow/cyan. The isovalue for the electronic spin density is roughly $10^{-7}$ e/Å$^3$ in both cases.

## Electronic surface properties of Ag(111)

To utterly describe the organometallic interface, the Ag properties must be investigated as well. Moreover, their knowledge will help us better understand the Kondo effect. In the following, we are interested in the modifications of the Ag surface properties when a very small amount of molecules is adsorbed such as in Fig. 1(b). To begin with, we have recorded a dI/dV curve on pristine Ag(111) prior to molecular adsorption. It is shown as a grey dashed curve in Fig.5(a). Its lineshape and energy onset is typical of the well-known Ag Shockley surface state.[68,106,107] After molecular adsorption at low coverage, a dI/dV spectra have been recorded on the uncovered Ag surface in between molecules. They are quite different compared to the one observed on the pristine Ag surface and they depend strongly on the location where they were recorded. Spectra 2 to 4 are given in Fig.5(a) as examples. The spectra can be described as a step-like lineshape with prominent peaks superimposed to it. As will be explained below, those extra peaks are eigenstates resulting from electron confinement. STM and conductance maps are shown in Fig.5(c-f). A strong spatially textured background between the molecules is observed for energies $eV_b$ above the Ag Shockley state energy onset $E_0$. This is illustrated by the STM image recorded at $-40$ meV in Fig.5(b). The effect is even better evidenced on the three conductance maps shown in Fig.5(c-f). Indeed, whereas the dI/dV map recorded at $-0.1$ V in (c) shows a constant and homogeneous background, strong variation of the conductance is observed on the flat areas of bare Ag between the molecules for the map at $eV_b > E_0$ in Fig.5(d-f). Moreover, it depends strongly on the energy. Due to these characteristics, we attribute these observations to the formation of standing wave patterns resulting from the scattering of the 2D nearly free electron surface state of Ag. In other words, 2HPc molecules act as electron scatterers of nanometric size.

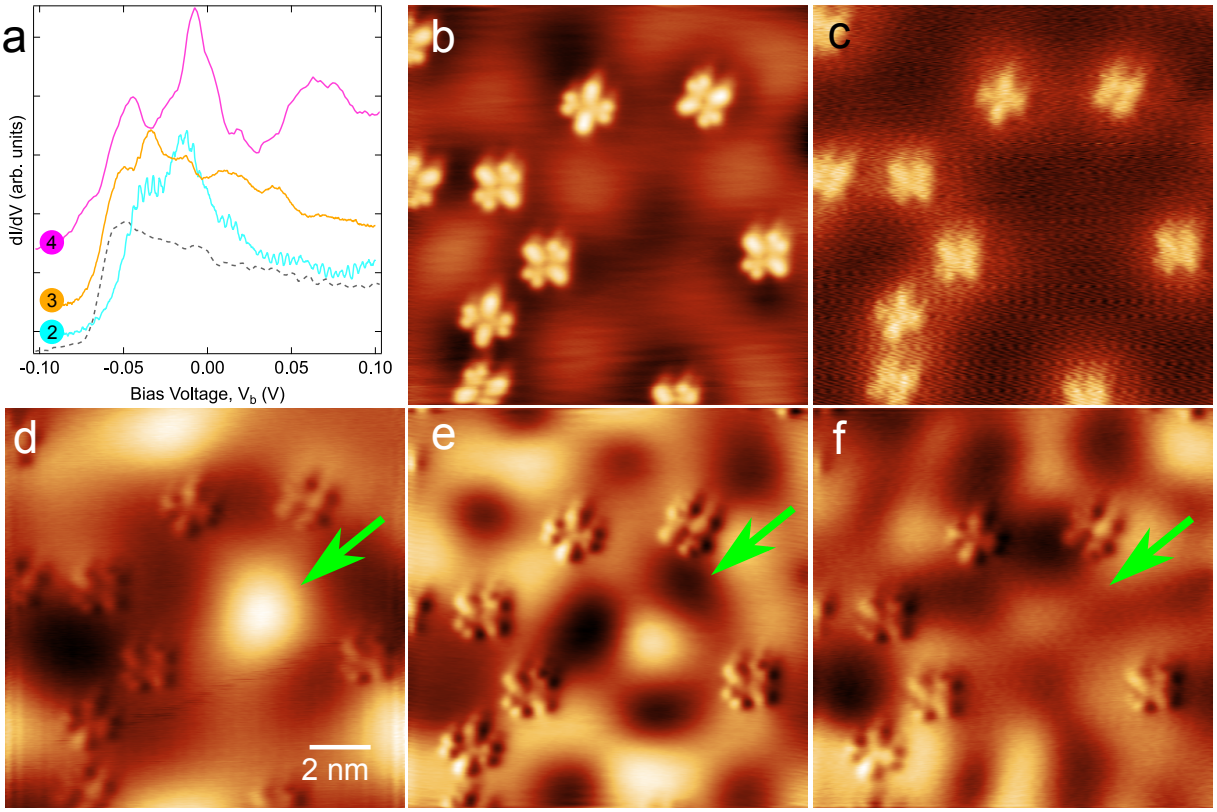


Figure 5: Electronic properties of Ag in G-phase. (a) dI/dV spectra recorded on Ag(111) between molecules in solid lines and on a pristine Ag(111) surface in dashed line. Numerical labels 2 to 4 correspond to the position of the tip marked by a matching colored cross in Fig.1(c) and Fig.S4(b). Tunneling bias conditions: $V_b = -1.8$ V, $I_t = 200$ pA. (b) STM topographic image. Tunneling bias conditions: $V_b = -40$ mV, $I_t = 200$ pA, (c-f) dI/dV maps recorded at $-100$ mV,$-40$ mV,$+10$ mV and $+30$ mV, respectively. Tunneling current $I_t = 200$ pA.

On those maps, the most surprising feature is the one observed at the center of the image as pointed by the green arrow in Fig.5(d-f) that is reminiscent of electron confinement in closed 2D artificial hexagonal Ag nanovacancies,[108] nanoislands[109–111] or even 2D porous molecular networks adsorbed on coinage (111) metal surfaces.[112] What is remarkable is that, contrary to those 2D resonators that are closed structures delimited by hard walls, the pattern of this current work have been obtained with only 4 or 5 molecules that are 2 to 5 nm apart and thus forming an open structure. In the abovementioned examples of electron confinement, the potential barrier is con-

sidered as continuous whereas it is obviously discontinuous in the present work. Shchyrba;et al. showed previously partial confinement insides molecular pores with missing borders.[113] Pennec;et al. showed confinement of the Ag surface state in a U-shaped cavity formed of linear molecular walls. However, to the best of our knowledge, the formation of an open walls molecular confining cavity has not been evidenced yet and therefore deserves a keen interest.

Scattering of the surface state of (111) surfaces of coinage metals by $\pi$- conjugated molecules have been previously observed.[114–118] When self-assembled in specific ways such as in Ref.[117] or organized in metal-organic frameworks, molecules can act as scattering walls for electrons of a two-dimensional electron gas. Quantum well arrays can thus be formed with well-defined molecular boundaries. Single $\pi$-conjugated molecular scatterer has been modeled[114] as a collection of atomic total absorbers at the position of the carbon atoms using multiple scattering expansion as developped for quantum corrals.[119] In molecular porous networks, scattering molecules are described in the framework of the boundary elements method where molecular boundaries correspond to constant rectangular potential.[116] The case of 2HPc on Ag(111) at low coverage is singular in the sense that it represents an intermediate case between the two situations cited above. Therefore, to explain the patterns observed in our work, a complementary theoretical approach might be necessary and further experimental investigations are required. This demonstrates that the 2HPc/Ag(111) interface offers the possibility to explore new fundamental aspects of quantum physics *i.e*. the electron scattering by an object of nanometric size composed of a collection of atomic-like scatterers covalently bonded. Besides, it holds promise for the design of tunable low-dimensional electron resonator. As will be discussed in section V, quantum confinement might have a non negligible impact on the Kondo effect.

## Discussion

In this section, we would like to address the mechanism behind the variation of $T_K$ within the G-phase as well as with molecular density. In previous sections we have shown that $T_K$ for single molecules can vary by about several tens of K. In addition, it is about twice smaller in the C-phase

as compared with the G-phase.

**Prior to that, the question arises whether the UPS spectra of the two phases corroborate STS results? To answer this question, a quantitative extraction of $T_K$ would be necessary. However, such analysis requires a temperature dependence of the linewidth of the Kondo peak together with theoretical calculations of the spectral function.[120] Solely based on (i) the width and intensity of the Kondo resonance which are larger for the C-phase than for the G-phase, (ii) theoretical descriptions of the variation of the spectral function[87] and (iii) experimental photoemission intensity of heavy fermions systems as a function of $T_K$ ,[87,89,90,120] we would conclude that the C-phase has a higher $T_K$ than the G-phase. This would contradict our STS measurements. However, in the present case, a direct parallel with those available works on strongly correlated materials is not totally valid since the $\pi$-orbital is involved instead of $4f$ states. In addition, here, electron-vibron coupling related to vibrational energies very close to $E_F$ is present. The presence of such a coupling might result in satellite Kondo resonances at energies related to $E_\nu$ and therefore might contribute to the width of the UPS spectra in the close vicinity of $E_F$ .[98] The intensity of the coupling is likely to vary between the two phases thus affecting differently the intensity and the width of the corresponding resonances. Further theoretical work is required to properly describe molecular vibrational Kondo effect and to analyze experimental UPS lineshape when charge-vibron coupling is present in a Kondo system. As a conclusion, the following discussion can only be based on $T_K$ extracted from STS.**

The Kondo temperature inside the G-phase can be assumed to depend on the adsorption configuration.[53] Nevertheless, it is not supported by our DFT calculations: adsorption heights and PDOS are very similar for both $\alpha$ and $\beta$ configurations. Comparing G and C-phase, a possible explanation could lie in the effect of intermolecular interactions. It has been shown in some Pc supramolecular assemblies that ligand-ligand interaction could engender a lifting of the molecules, reducing the molecule-substrate coupling and thus, $T_K$ .[28,56] However, according to our DFT calculations, the adsorption height varies only minutely between the two phases. In addition, as shown in Fig.S6

in the Supporting Information, the PDOS of the 2HPc molecule on Ag(111) at low concentration is very similar to the one of molecules in the C-phase reported in Fig.4(d). The position of the F-LUMO varies only a little and a charge transfer of $0.27$ electrons has been extracted. This is very close to the value of $0.32$ electrons obtained for the self-assembly. This supposes that the coupling strength with the substrate doesn't vary much upon formation of the C-phase and can not account for the strong variation of $T_K$ .

The Ruderman-Kittel-Kasuya-Yoshida (RKKY) interaction is an alternative origin. It is an indirect spin-spin interaction mediated by the conduction electrons of the metal. Depending on distance, it favours ferromagnetic or antiferromagnetic (AFM) alignments of single magnetic moments. It has been shown that an interplay between the Kondo effect and the RKKY interaction exists in supramolecular assemblies, as well.[52,62] The width of the Abrikosov-Suhl resonance is strongly affected or even suppressed due to the magnetic coupling between the spins. More specifically, FM RKKY interaction sharpens the resonance and, on the other hand, the AFM RKKY broadens it.[121] Unfortunately, it is very challenging to test the assumption whether RKKY interaction is responsible for the reduction of $T_K$ in the self-assembly. Indeed, in order to demonstrate it, a thought experiment would be to measure $T_K$ by STS as a function of the molecule-molecule distance for a pair of molecules to mimic the conditions of the two-impurities Kondo problem.[122] However, in such a case of a molecular pair, surface electrons would dominate the RKKY interaction due to their lower $k_F$ compared to bulk electrons and couldn't be used to conclude on the exchange coupling in the self-assembly for which the surface state has hybridized with a molecular orbital to form the unoccupied HIS. Nevertheless, one can tentitatively apply the following formula to predict the sign of the exchange coupling in the commensurate phase: $J = J_0 \frac{sin(2k_F r)}{(2k_F r)^2}$, where $k_F$ is the Fermi wave vector of the substrate and $r$, the distance between the spins. The latter parameter $r$ can be estimated from the calculated lattice parameters of the rectangular unit cell (black dashed line in Fig. 2(c)) that are equal to $1.51$ nm and $1.45$ nm) and $k_F = 12.02\,\mathrm{nm}^{-1}$.[123] Moreover, we discard the influence of the second-nearest neighbors due to the fast decay of the exchange for bulk electrons. The result gives an AFM coupling between nearest-neighbors molecules. This

would lead to an increase of $T_K$ compared with the single impurity case which contradicts our experimental findings. Therefore RKKY can not account for the decrease of $T_K$ upon formation of self-assembly.

The observed variation of $T_K$ between the two phases could be alternatively explained considering that $T_K$ is directly proportional to $\exp^{\frac{-1}{\rho_F J}}$, where $\rho_F$ is the substrate's density of states at the Fermi energy and J is the exchange coupling at the magnetic impurity.[87] This relationship indicates that when $\rho_F$ is reduced, $T_K$ is reduced as a result. At low molecular concentration, the uncovered substrate exhibits a Shockley surface state that participates to $\rho_F$. In the case of the C-phase, as this state hybridizes with the LUMO state of the free molecule to form the HIS shifted above $E_F$, $\rho_F$ is reduced in comparison with the isolated molecules and thus, would explain the decrease of $T_K$ for the C-phase.

The influence of the surface state on the Kondo resonance width has been a topic of debate for many years (see Ref.[124] and references therein). Some works on Ag(111) have suggested a minor role for surface-state electrons in the Kondo effect.[125] Only very recently, Li;et al. tackle this controversy using LT-STM/STS on Co adsorbates on Ag(111).[124] They unambiguously demonstrate the influence of the surface state on the Kondo resonance by measuring the width of the zero-bias peak as a function of the lateral distance to the impurity. The key point is that they evidenced an oscillatory dependency as a function of the distance to the magnetic impurity which periodicity matches the half Fermi wavelength of the Ag(111) surface state. Moro-Lagares;et al. obtained experimentally and theoretically a nearly linear relationship between $T_K$ and the surface-state contribution local density of states of the substrate.[126] Besides, both works emphasize the effect of quantum confinement of the surface state. In particular, it was evidenced that in a quantum corral, the Kondo width can be significantly increased (more than three times).[124] As at low molecular density in the 2HPc/Ag(111) system, quantum confinement of the Ag surface state is also observed, it probably also plays a significant role on the high value of $T_K$ and its variation in the G-phase. The effect of the Shockley surface state on $T_K$ has also been observed on molecules such as Co-tetraphenylporphirin on Cu(111).[115] In this work, Iancu;et al. showed that molecules

exposed to Cu surface state electrons exhibit a higher $T_K$ than molecules inside a self-assembled cluster. These results are in favor of our observation of a lower $T_K$ upon self-assembly.

# CONCLUSIONS

As a conclusion, we have studied the electronic properties of the metal-free phthalocyanine 2HPc adsorbed on Ag(111) surfaces by means of scanning tunneling and photoelectron spectroscopies and compared the experimental results with DFT calculations. We have evidenced a partial filling of a molecular $\pi$ state lying next to the Fermi level. The presence of this extra $\pi$-spin in the molecule leads to the emergence of a Kondo effect at low temperature for single molecules as well as for molecules arranged in a 2D self-assembly.

The fact that we deal with a metal-free phthalocyanine offer many future prospects. In other words, the absence of a metal ion at the center of the molecule is the asset of this system. Indeed, it has been shown that this metal free central cavity of 2HPc can be manipulated by STM in many ways: tautomerization[84], partial or total deshydrogenation or direct Ag metalation can be induced.[46] Therefore, one can envisage to investigate the influence of such modifications on the Kondo physics. As an example, a 2HPc molecule can be transformed into an AgPc molecule in the self-assembly[46] and study the effect on $T_K$. In that case, $T_K$ is likely to change through the modification of the local coupling with the substrate via the up or down-lifting of the molecules or the RKKY interaction between neighbouring molecules.

Besides the STM manipulation-based approach, local modification of the electronic and magnetic properties of 2HPc can be obtained by on- surface synthesis such as chemical doping or metallation upon adsorption of alkali or metallic atoms under UHV.[26,85] Using Li dopants, the charge transfer could be locally modulated and the molecular spin could be tuned[26]. In another study, Bai;et al. showed that 2HPc react strongly with Fe atoms to form FePc molecules on Ag(111).[85] This on-surface metalation process was theoretically shown to be energetically favorable for M=Co, Ni, Mn on 2HPc/Ag(111).[127] It would be particularly interesting to study the

Kondo physics in the MPc/2HPc hetero-molecular arrays as a function of MPc concentration. Overall, any combination of the above cited manipulation strategies might be used. For these reasons, this system offers an exceptionnaly rich playground for investigating the molecular Kondo physics.

**Supporting Information Available**

STS spectra of G and C-phases and Fano fits. Calculated band structure of Ag. Sequence of STM images showing in-plane molecular rotation. UPS spectra of G and C-phases. Computed density of states projected onto atomic orbitals of 2HPc molecules on Ag(111) assembled in a $7 \times 7$ arrangement. Details on tip conditions for the observation of the Kondo resonance in STS spectra.

This material is available free of charge via the Internet at http://pubs.acs.org.

# References


1. Urtizberea, A.; Natividad, E.; Alonso, P. J.; Andrés, M. A.; Gascón, I.; Goldmann, M.; Roubeau, O. A Porphyrin Spin Qubit and Its 2D Framework Nanosheets, *Adv. Funct. Mater* **2018**, *28*,1801695–15.

2. Gaita-Ariño, A.; Luis, F.; Hill, S.; Coronado, E. Molecular Spins for Quantum Computation, *Nat. Chem.* **2019**, *11*, 301–309.

3. Cavallini, M.; Gomez-Segura, J.; Ruiz-Molina, D.; Massi, M.; Albonetti, C.; Rovira, C.; Veciana, J.; Biscarini, F. Magnetic Information Storage on Polymers by Using Patterned Single-Molecule Magnets, *Angew. Chem., Int. Ed.* **2005**,*44*,888–892.

4. Cinchetti, M.; Dediu, V. A.; Hueso, L. E. Activating the Molecular Spinterface, *Nat. Mater.* **2017,** *16*, 507–515

5. Bogani, L.; Wernsdorfer, W. Molecular Spintronics Using Single-Molecule Magnets, *Nat. Mater.* **2008**, *7*, 179–186

6. Mannini, M.; Pineider, F.; Sainctavit, P.; Danieli, C.; Otero, E.; Sciancalepore, C.; Talarico, A. M.; Arrio, M.-A.; Cornia, A.; Gatteschi, D.; et al. Magnetic Memory of a Single-Molecule Quantum Magnet Wired to a Gold Surface, *Nat. Mater.* **2009**, *8*, 194–197.

7. Guo, F.-S.; Day, B. M.; Chen, Y.-C.; Tong, M.-L.; Mansikkamäki, A.; Layfield, R. A. A Dysprosium Metallocene Single-Molecule Magnet Functioning at the Axial Limit, *Angew. Chem., Int. Ed.* **2017**, *56*, 11445–11449.

8. Zhao, A.; Li, Q.; Chen, L.; Xiang, H.; Wang W.; Pan, S.; Wang B.; Xiao, X.; Yang, J.; Hou, J. G.; and Zhu, Q. Controlling the Kondo Effect of an Adsorbed Magnetic Ion Through Its Chemical Bonding, *Science* **2005**, *309*, 1542–1544.

9. Li, Z.; Li, B.; Yang, J.; Hou, J. G. Single-Molecule Chemistry of Metal Phthalocyanine on Noble Metal Surfaces, *Acc. Chem. Res.* **2010**, *43*, 954–962.

10. Niu, T.; Li, A. Exploring Single Molecules by Scanning Probe Microscopy: Porphyrin and Phthalocyanine, *J. Phys. Chem. Lett.* **2013**, *4*, 4095–4102.

11. Komeda, T.; Katoh, K.; Yamashita, M. Double-decker phthalocyanine complex: Scanning Tunneling Microscopy Study of Film Formation and Spin Properties, *Prog.in Surf. Sci.* **2014**, *89*, 127–160.

12. Ishikawa, N.; Sugita, M.; Ishikawa, T.; Koshihara, S.; Kaizu, Y. Lanthanide Double-Decker Complexes Functioning as Magnets at the Single-Molecular Level, *J. Am. Chem. Soc.* **2003**, *125*, 8694–8695.

13. Ishikawa, N.; Sugita, M.; Wernsdorfer, W. Quantum Tunneling of Magnetization in Lanthanide Single-Molecule Magnets: Bis(phthalocyaninato)terbium and Bis(phthalocyaninato)dysprosium Anions, *Angew. Chem., Int. Ed.* **2005**, *44*, 2931–2935.

14. Urdampilleta, M.; Klyatskaya, S.; Cleuziou, J.-P.; Ruben, M.; Wernsdorfer, W. Supramolecular Spin Valves, *Nat. Mater.* **2011**, *10*, 502–506.

15. Gottfried, J. M. Surface Chemistry of Porphyrins and Phthalocyanines, *Surf. Sci. Reports* **2015**, *70*, 259–379.

16. Amsterdam, S. H.; Stanev, T. K.; Zhou, Q.; Lou, A. J. T.; Bergeron, H.; Darancet, P.; Hersam, M. C.; Stern, N. P.; Marks, T. J. Electronic Coupling in Metallophthalocyanine–Transition Metal Dichalcogenide Mixed-Dimensional Heterojunctions, *ACS Nano* **2019**, *13*, 4183–4190.

17. Kafle, T. R.; Kattel, B.; Lane, S. D.; Wang, T.; Zhao, H.; Chan, W.-L. Charge Transfer Exciton and Spin Flipping at Organic–Transition-Metal Dichalcogenide Interfaces, *ACS Nano* **2017**, *11*, 10184–10192.

18. Padgaonkar, S.; Amsterdam, S. H.; Bergeron, H.; Su, K.; Marks, T. J.; Hersam, M. C.; Weiss, E. A. Molecular Orientation-Dependent Interfacial Charge Transfer in Phthalocyanine/MoS2 Mixed-Dimensional Heterojunctions, *J. Phys. Chem. C* **2019**, *123*, 13337–13343.

19. Suzuki, T.; Kurahashi, M.; Ju, X.; Yamauchi, Y. Spin Polarization of Metal (Mn, Fe, Cu, and Mg) and Metal-Free Phthalocyanines on an Fe(100) Substrate, *J. Phys. Chem. B* **2002**, *106*, 11553–11556.

20. Atodiresei, N.; Brede, J.; Lazić, P.; Caciuc, V.; Hoffmann, G.; Wiesendanger, R.; Blügel, S. Design of the Local Spin Polarization at the Organic-Ferromagnetic Interface, *Phys. Rev. Lett.* **2010**, *105*, 066601.

21. Djeghloul, F.; Gruber, M.; Urbain, E.; Xenioti, D.; Joly, L.; Boukari, S.; Arabski, J.; Bulou, H.; Scheurer, F.; Bertran, F.; et al. High Spin Polarization at Ferromagnetic Metal–Organic Interfaces: A Generic Property, *J. Phys. Chem. Lett.* **2016**, *7*, 2310–2315.

22. Delprat, S.; Galbiati, M.; Tatay, S.; Quinard, B.; Barraud, C.; Petroff, F.; Seneor, P.; Mattana, R. Molecular Spintronics: the Role of Spin-Dependent Hybridization, *J. Phys. D: Appl. Phys.* **2018**, *51*, 473001.

23. Caputo, M.; Panighel, M.; Lisi, S.; Khalil, L.; Santo, G. D.; Papalazarou, E.; Hruban, A.; Konczykowski, M.; Krusin-Elbaum, L.; Aliev, Z. S.; et al. Manipulating the Topological Interface by Molecular Adsorbates: Adsorption of Co-Phthalocyanine on Bi2Se3, *Nano Lett.* **2016**, *16*, 3409–3414.

24. Bauer, J.; Pascual, J. I.; Franke, K. J. Microscopic Resolution of the Interplay of Kondo Screening and Superconducting Pairing: Mn-Phthalocyanine Molecules Adsorbed on Superconducting Pb(111), *Phys. Rev. B* **2013**, *87*, 075125.

25. Malavolti, L.; Briganti, M.; Hänze, M.; Serrano, G.; Cimatti, I.; McMurtrie, G.; Otero, E.; Ohresser, P.; Totti, F.; Mannini, M.; et al. Tunable Spin–Superconductor Coupling of Spin 1/2 Vanadyl Phthalocyanine Molecules, *Nano Lett.* **2018**, *18*, 7955–7961.

26. Krull, C.; Robles, R.; Mugarza, A.; Gambardella, P. Site- and Orbital-Dependent Charge Donation and Spin Manipulation in Electron-Doped Metal Phthalocyanines, *Nat. Mater.* **2013**, *12*, 337–343.

27. Ballav, N.; Wäckerlin, C.; Siewert, D.; Oppeneer, P. M.; Jung, T. A. Emergence of On-Surface Magnetochemistry, *J. Phys. Chem. Lett.* **2013**, *4*, 2303–2311.

28. Mugarza, A.; Krull, C.; Robles, R.; Stepanow, S.; Ceballos, G.; Gambardella, P. Spin Coupling and Relaxation Inside Molecule–Metal Contacts, *Nat. Comm.* **2011**, *2*, 490.

29. Mugarza, A.; Robles, R.; Krull, C.; Korytár, R.; Lorente, N.; Gambardella, P. Electronic and Magnetic Properties of Molecule-Metal Interfaces: Transition-Metal Phthalocyanines Adsorbed on Ag(100), *Phys. Rev. B* **2012**, *85*, 155437–13.

30. Anderson, P. W. Localized Magnetic States in Metals, *Phys. Rev.* **1961**, *124*, 41–53.

31. Kondo, J. Resistance Minimum in Dilute Magnetic Alloys, *Prog. Theor. Phys.* **1964**, *32*, 37–49.

32. Li, J.; Schneider, W.-D.; Berndt, R.; Delley, B. Kondo Scattering Observed at a Single Magnetic Impurity, *Phys. Rev. Lett.* **1998**, *80*, 2893–2896.

33. Madhavan, V.; Chen, W.; Jamneala, T.; Crommie, M. F.; Wingreen, N. S. Tunneling into a Single Magnetic Atom: Spectroscopic Evidence of the Kondo Resonance, *Science* **1998**, *280*, 567–569.

34. Komeda, T. Spins of Adsorbed Molecules Investigated by the Detection of Kondo Resonance, *Surf. Sci.* **2014**, *630*, 343–355.

35. Ternes, M.; Heinrich, A. J.; Schneider, W.-D. Spectroscopic Manifestations of the Kondo Effect on Single Adatoms, *J. Phys.: Condens. Matter* **2008**, *21*, 053001.

36. Toader, M.; Shukrynau, P.; Knupfer, M.; Zahn, D. R. T.; Hietschold, M. Site-Dependent Donation/Backdonation Charge Transfer at the CoPc/Ag(111) Interface, *Langmuir* **2012**, *28*, 13325–13330.

37. Gorgoi, M.; Zahn, D. R. Charge-Transfer at Silver/Phthalocyanines Interfaces, *Appl. Surf. Sci.* **2006**, *252*, 5453–5456.

38. Kröger, I.; Bayersdorfer, P.; Stadtmüller, B.; Kleimann, C.; Mercurio, G.; Reinert, F.; Kumpf, C. Submonolayer Growth of H2-Phthalocyanine on Ag(111), *Phys. Rev. B* **2012**, *86*, 195412.

39. Caplins, B. W.; Suich, D. E.; Shearer, A. J.; Harris, C. B. Metal/Phthalocyanine Hybrid Interface States on Ag(111), *J. Phys. Chem. Lett.* **2014**, *5*, 1679–1684.

40. Fernández-Torrente, I.; Franke, K. J.; Pascual, J. I. Vibrational Kondo Effect in Pure Organic Charge-Transfer Assemblies, *Phys. Rev. Lett.* **2008**, *101*, 217203.

41. Choi, T.; Bedwani, S.; Rochefort, A.; Chen, C.-Y.; Epstein, A. J.; Gupta, J. A. A Single Molecule Kondo Switch: Multistability of Tetracyanoethylene on Cu(111), *Nano Lett.* **2010**, *10*, 4175–4180.

42. Liu, J.; Isshiki, H.; Katoh, K.; Morita, T.; Brian, K. B.; Yamashita, M.; Komeda, T. First Observation of a Kondo Resonance for a Stable Neutral Pure Organic Radical, 1,3,5-Triphenyl-6-oxoverdazyl, Adsorbed on the Au(111) Surface, *J. Am. Chem. Soc.* **2012**, *135*, 651–658.

43. Requist, R.; Modesti, S.; Baruselli, P. P.; Smogunov, A.; Fabrizio, M.; Tosatti, E. Kondo Conductance Across the Smallest Spin 1/2 Radical Molecule, *Proc. Natl. Acad. Sci.* **2013**, *111*, 69–74.

44. Esat, T.; Lechtenberg, B.; Deilmann, T.; Wagner, C.; Krüger, P.; Temirov, R.; Rohlfing, M.; Anders, F. B.; Tautz, F. S. A Chemically Driven Quantum Phase Transition in a Two-Molecule Kondo System, *Nat. Phys.* **2016**, *12*, 867–873.

45. Karan, S.; Li, N.; Zhang, Y.; He, Y.; Hong, I.-P.; Song, H.; Lü, J.-T.; Wang, Y.; Peng, L.; Wu, K. ;et al. Spin Manipulation by Creation of Single-Molecule Radical Cations, *Phys. Rev. Lett.* **2016**, *116*, 027201.

46. Sperl, A.; Kröger, J.; Berndt, R. Controlled Metalation of a Single Adsorbed Phthalocyanine, *Angew. Chem., Int. Ed.* **2011**, *50*, 5294–5297.

47. Perera, U. G. E.; Kulik, H. J.; Iancu, V.; da Silva, L. G. G. V. D.; Ulloa, S. E.; Marzari, N.; Hla, S.-W. Spatially Extended Kondo State in Magnetic Molecules Induced by Interfacial Charge Transfer,*Phys. Rev. Lett.* **2010**, *105*, 106601.

48. Booth, C. H.; Walter, M. D.; Daniel, M.; Lukens, W. W.; Andersen, R. A. Self-Contained Kondo Effect in Single Molecules, *Phys. Rev. Lett.* **2005**, *95*, 267202.

49. Wahl, P.; Diekhöner, L.; Wittich, G.; Vitali, L.; Schneider, M. A.; Kern, K. Kondo Effect of

Molecular Complexes at Surfaces: Ligand Control of the Local Spin Coupling, *Phys. Rev. Lett.* **2005**, *95*, 166601.

50. Zhao, A.; Hu, Z.; Wang, B.; Xiao, X.; Yang, J.; Hou, J. G. Kondo Effect in Single Cobalt Phthalocyanine Molecules Adsorbed on Au(111) Monoatomic Steps ‚*J. Chem. Phys.* **2008**, *128*, 234705.

51. Scott, G. D.; Natelson, D. Kondo Resonances in Molecular Devices, *ACS Nano* **2010**, *4*, 3560–3579.

52. Tsukahara, N.; Shiraki, S.; Itou, S.; Ohta, N.; Takagi, N.; Kawai, M. Evolution of Kondo Resonance from a Single Impurity Molecule to the Two-Dimensional Lattice, *Phys. Rev. Lett.* **2011**, *106*, 187201.

53. Minamitani, E.; Tsukahara, N.; Matsunaka, D.; Kim, Y.; Takagi, N.; Kawai, M. Symmetry-Driven Novel Kondo Effect in a Molecule, *Phys. Rev. Lett.* **2012**, *109*, 086602.

54. Ziroff, J.; Hame, S.; Kochler, M.; Bendounan, A.; Schöll, A.; Reinert, F. Low-Energy Scale Excitations in the Spectral Function of Organic Monolayer Systems, *Phys. Rev. B* **2012**, *85*, 161404.

55. Garnica, M.; Stradi, D.; Barja, S.; Calleja, F.; Díaz, C.; Alcamí, M.; Martín, N.; de Parga, A. L. V.; Martín, F.; Miranda, R. Long-Tange Magnetic Order in a Purely Organic 2D Layer Adsorbed on Epitaxial Graphene, *Nat. Phys.* **2013**, *9*, 368–374.

56. Komeda, T.; Isshiki, H.; Liu, J.; Katoh, K.; Shirakata, M.; Breedlove, B. K.; Yamashita, M. Variation of Kondo Peak Observed in the Assembly of Heteroleptic 2,3-Naphthalocyaninato Phthalocyaninato Tb(III) Double-Decker Complex on Au(111), *ACS Nano* **2013**, *7*, 1092–1099.

57. Iancu, V.; Braun, K.-F.; Schouteden, K.; Haesendonck, C. V. Inducing Magnetism in Pure Organic Molecules by Single Magnetic Atom Doping, *Phys. Rev. Lett.* **2014**, *113*, 106102.

58. Lin, T.; Kuang, G.; Wang, W.; Lin, N. Two-Dimensional Lattice of Out-of-Plane Dinuclear Iron Centers Exhibiting Kondo Resonance, *ACS Nano* **2014**, *8*, 8310–8316.

59. Zhang, Q.; Kuang, G.; Pang, R.; Shi, X.; Lin, N. Switching Molecular Kondo Effect via Supramolecular Interaction, *ACS Nano* **2015**, *9*, 12521–12528.

60. Maughan, B.; Zahl, P.; Sutter, P.; Monti, O. L. A. Ensemble Control of Kondo Screening in Molecular Adsorbates, *J. Phys. Chem. Lett.* **2017**, *8*, 1837–1844.

61. Hiraoka, R.; Minamitani, E.; Arafune, R.; Tsukahara, N.; Watanabe, S.; Kawai, M.; Takagi, N. Single-molecule quantum dot as a Kondo simulator, *Nat. Comm.* **2017**, *8*, 1–7.

62. Tuerhong, R.; Ngassam, F.; Watanabe, S.; Onoe, J.; Alouani, M.; Bucher, J.-P. Two-Dimensional Organometallic Kondo Lattice with Long-Range Antiferromagnetic Order, *J. Phys. Chem. C* **2018**, *122*, 20046–20054.

63. Temirov, R.; Soubatch, S.; Luican, A.; Tautz, F. S. Free-Electron-Like Dispersion in an Organic Monolayer Film on a Metal Substrate, *Nature* **2006**, 444, 350–353.

64. Armbrust, N.; Schiller, F.; Güdde, J.; Höfer, U. Model Potential for the Description of Metal/Organic Interface States, *Sci. Rep.* **2017**, *7*, 1–8.

65. Lerch, A.; Fernandez, L.; Ilyn, M.; Gastaldo, M.; Paradinas, M.; Valbuena, M. A.; Mugarza, A.; Ibrahim, A. B. M.; Sundermeyer, J.; Höfer, U.; et al. Electronic Structure of Titanylphthalocyanine Layers on Ag(111) , *J. Phys. Chem. C* **2017**, *121*, 25353–25363.

66. Gerbert, D.; Hofmann, O. T.; Tegeder, P. Formation of Occupied and Unoccupied Hybrid Bands at Interfaces between Metals and Organic Donors/Acceptors, *J. Phys. Chem. C*, **2018**, *122*, 27554–27560.

67. Sabitova, A.; Temirov, R.; Tautz, F. S. Lateral Scattering Potential of the PTCDA/Ag(111) Interface State, *Phys. Rev. B*, **2018**, *98*, 205429.

68. Bürgi, L.; Knorr, N.; Brune, H.; Schneider, M.; Kern, K. Two-Dimensional Electron Gas at Noble-Metal Surfaces, *Appl. Phys. A: Mater. Sci. Process.* **2002** , *75* , 141–145.

69. Reinert, F.; Nicolay, G.; Schmidt, S.; Ehm, D.; Hüfner, S. Direct Measurements of the L-gap Surface States on the (111) Face of Noble Metals by Photoelectron Spectroscopy, *Phys. Rev. B* **2001**, *63*, 115415

70. Puschnig, P.; Berkebile, S.; Fleming, A. J.; Koller, G.; Emtsev, K.; Seyller, T.; Riley, J. D.; Ambrosch-Draxl, C.; Netzer, F. P.; Ramsey, M. G. Reconstruction of Molecular Orbital Densities from Photoemission Data, *Science* **2009**, *326*, 702–706.

71. Gargiani, P.; Betti, M. G.; Taleb-Ibrahimi, A.; Le Fèvre, P.; Modesti, S. Orbital Symmetry of the Kondo State in Adsorbed FePc Molecules on the Au(110) Metal Surface, *J. Phys. Chem. C* **2016**, *117*, 26144–26155.

72. Kresse, G.; Hafner, J. Physical Review B **1993**, *47*, 558–561.

73. Kresse, G.; Hafner, J. Ab Initio Molecular Dynamics for Liquid Metals, *Phys. Rev. B* **1994**, *49*, 14251–14269.

74. Kresse, G.; Furthmüller, J. Efficient Iterative Schemes for Ab Initio Total-Energy Calculations Using a Plane-Wave Basis Set, *Phys. Rev. B* **1996**, *54*, 11169–11186.

75. Kresse, G.; Furthmüller, J. Efficiency of Ab-Initio Total Energy Calculations for Metals and sSemiconductors Using a Plane-Wave Basis Set, *Comput. Mater. Sci.* **1996**, *6*, 15–50.

76. Blöchl, P. E. Projector Augmented-Wave Method, *Phys. Rev. B* **1994**, *50*, 17953–17979.

77. Kresse, G.; Joubert, D. From Ultrasoft Pseudopotentials to the Projector Augmented-Wave Method, *Phys. Rev. B* **1999**, *59*, 1758–1775.

78. Perdew, J. P.; Burke, K.; Ernzerhof, M. Generalized Gradient Approximation Made Simple, *Phys. Rev. Lett.* **1996**, *77*, 3865–3868.

79. Grimme, S.; Antony, J.; Ehrlich, S.; Krieg, H. A Consistent and Accurate Ab Initio Parametrization of Density Functional Dispersion Correction (DFT-D) for the 94 elements H-Pu, *J. Chem. Phys.*, **2010**, *132*, 154104.

80. Bučko, T.; Hafner, J.; Lebègue, S.; Ángyán, J. G. Improved Description of the Structure of Molecular and Layered Crystals: Ab Initio DFT Calculations with van der Waals Corrections, *J. Phys. Chem. A* **2010**, *114*, 11814–11824.

81. Huang, Y.; Wruss, E.; Egger, D.; Kera, S.; Ueno, N.; Saidi, W.; Bucko, T.; Wee, A.; Zojer, E. Understanding the Adsorption of CuPc and ZnPc on Noble Metal Surfaces by Combining Quantum-Mechanical Modelling and Photoelectron Spectroscopy, *Molecules* **2014**, *19*, 2969–2992.

82. Blöchl, P. E.; Jepsen, O.; Andersen, O. K. Improved Tetrahedron Method for Brillouin-Zone Integrations, *Phys. Rev. B* **1994**, *49*, 16223–16233.

83. Zaitsev, N. L.; Nechaev, I. A.; Echenique, P. M.; Chulkov, E. V. Transformation of the Ag(111) Surface State Due to Molecule-Surface Interaction with Ordered Organic Molecular Monolayers *Phys. Rev. B* **2012**, *85*, 115301.

84. Kügel, J.; Sixta, A.; Böhme, M.; Krönlein, A.; Bode, M. Breaking Degeneracy of Tautomerization—Metastability from Days to Seconds, *ACS Nano* **2016**, *10*, 11058–11065.

85. Bai, Y.; Buchner, F.; Wendahl, M. T.; Kellner, I.; Bayer, A.; Steinrück, H.-P.; Marbach, H.; Gottfried, J. M. Direct Metalation of a Phthalocyanine Monolayer on Ag(111) with Coadsorbed Iron Atoms, *J. Phys. Chem. C* **2008**, *112*, 6087–6092.

86. Nilson, K.; Åhlund, J.; Shariati, M. N.; Schiessling, J.; Palmgren, P.; Brena, B.; Göthelid, E.; Hennies, F.; Huismans, Y.; Evangelista, F.; et al. Potassium-Intercalated H2Pc films: Alkali-Induced Electronic and Geometrical Modifications, *J. Phys. Chem. C* **2012**, *137*, 044708.

87. Hewson, A. C. The Kondo Problem to Heavy Fermions, Cambridge University Presse, Cambridge, UK **1993**

88. Nagaoka, K.; Jamneala, T.; Grobis, M.; Crommie, M. F. Temperature Dependence of a Single Kondo Impurity, *Phys. Rev. Lett.* **2002**, *88*, 1497.

89. Gunnarsson, O.; Schönhammer, K. Electron Spectroscopies for Ce Compounds in the Impurity Model, *Phys. Rev. B* **1983**, *28*, 4315–4341.

90. Malterre, D.; Grioni, M.; Baer, Y. Recent Developments in High-Energy Spectroscopies of Kondo Systems, *Adv.Phys.* **1996**, *45*, 299–348.

91. Bickers, N. E.; Cox, D. L.; Wilkins, J. W. Self-Consistent Large-N Expansion for Normal-State Properties of Dilute Magnetic Alloys, *Phys. Rev. B* **1987**, *36*, 2036–2079.

92. Patthey, F.; Imer, J.-M.; Schneider, W.-D.; Beck, H.; Baer, Y.; Delley, B. High-Resolution Photoemission Study of the Low-Energy Excitations in 4f-Electron Systems *Phys. Rev. B* **1990**, *42*, 8864–8881.

93. Costi, T. A. Kondo Effect in a Magnetic Field and the Magnetoresistivity of Kondo Alloys, *Phys. Rev. Lett.* **2000**, *85*, 1504–1507.

94. König, J.; Schoeller, H.; Schön, G. Zero-Bias Anomalies and Boson-Assisted Tunneling Through Quantum Dots, *Phys. Rev. Lett.* **1996**, *76*, 1715–1718.

95. Flensberg, K. Tunneling Broadening of Vibrational Sidebands in Molecular Transistors, *Phys. Rev. B* **2003**, *68*, 205323.

96. Paaske, J.; Flensberg, K. Vibrational Sidebands and the Kondo Effect in Molecular Transistors, *Phys. Rev. Lett.* **2005**, *94*, 176801.

97. Chen, Z.-Z.; Lu, H.; Lü, R.; fen Zhu, B. Phonon-Assisted Kondo Effect in a Single-Molecule Transistor out of Equilibrium, *J. Phys.: Condens. Matter* **2006**, *18*, 5435–5446.

98. Roura-Bas, P.; Tosi, L.; Aligia, A. A. Nonequilibrium Transport Through Magnetic Vibrating Molecules, *Phys. Rev. B* **2013**, *87*, 195136.

99. Parks, J. J.; Champagne, A. R.; Hutchison, G. R.; Flores-Torres, S.; Abruña, H. D.; Ralph, D. C. Tuning the Kondo Effect with a Mechanically Controllable Break Junction, *Phys. Rev. Lett.* **2007**, *99*, 026601.

100. Iancu, V.; Schouteden, K.; Li, Z.; Haesendonck, C. V. Electron–Phonon Coupling in Engineered Magnetic Molecules, *Chem. Comm.* **2016**, *52*, 11359–11362.

101. Endlich, M.; Gozdzik, S.; Néel, N.; da Rosa, A. L.; Frauenheim, T.; Wehling, T. O.; Kröger, J. Phthalocyanine Adsorption to Graphene on Ir (111): Evidence for Decoupling from Vibrational Spectroscopy, *J . Chem. Phys.* **2014**, *141*, 184308.

102. Fano, U. Effects of Configuration Interaction on Intensities and Phase Shifts, *Phys.l Rev.* **1961**, *124*, 1866–1878.

103. Gruber, M.; Weismann, A.; Berndt, R. The Kondo Resonance Line Shape in Scanning Tunnelling Spectroscopy: Instrumental Aspects, *J. Phys.: Condens. Matter* **2018**, *30*, 424001.

104. Bidermane, I.; Brumboiu, I. E.; Totani, R.; Grazioli, C.; Shariati-Nilsson, M. N.; Herper, H. C.; Eriksson, O.; Sanyal, B.; Ressel, B.; de Simone, M.; et al. Atomic Contributions to the Valence Band Photoelectron Spectra of Metal-Free, Iron and Manganese Phthalocyanines, *J. Electron Spectrosc. Relat. Phenom.* **2015**, *205*, 92–97.

105. Gerber, I. C.; Poteau, R. Critical Assessment of Charge Transfer Estimates in Non-Covalent Graphene Doping, *Theo. Chem. Acc.* **2018**, *137*, 156.

106. Li, J.; Schneider, W.-D.; Berndt, R. Local Density of States from Spectroscopic Scanning-Tunneling-Microscope Images: Ag(111), *Phys. Rev. B* **1997**, *56*, 7656–7659.

107. Jeandupeux, O.; Bürgi, L.; Hirstein, A.; Brune, H.; Kern, K. Thermal Damping of Quantum Interference Patterns of Surface-State Electrons, *Phys. Rev. B* **1999**, *59*, 15926–15934.

108. Jensen, H.; Kröger, J.; Berndt, R.; Crampin, S. Electron Dynamics in Vacancy Islands: Scanning Tunneling Spectroscopy on Ag(111), *Phys. Rev. B* **2005**, *71*, 155417.

109. Avouris, P.; Lyo, I.-W. Observation of Quantum-Size Effects at Room Temperature on Metal Surfaces With STM, *Science* **1994**, *264*, 942–945.

110. Li, J.; Schneider, W.-D.; Berndt, R.; Crampin, S. Electron Confinement to Nanoscale Ag Islands on Ag(111): A Quantitative Study, *Phys. Rev. Lett.* **1998**, *80*, 3332–3335.

111. Tournier-Colletta, C.; Kierren, B.; Fagot-Revurat, Y.; Malterre, D. Phonon Contribution to the Lifetime of Surface State Quasiparticles Confined in Nanopyramids, *Phys. Rev. Lett.* **2010**, *104*, 016802.

112. Müller, K.; Enache, M.; Stöhr, M. Confinement properties of 2D porous molecular networks on metal surfaces, *J. Phys.: Condens. Matter* **2016**, *28*, 153003.

113. Shchyrba, A.; Martens, S. C.; Wäckerlin, C.; Matena, M.; Ivas, T.; Wadepohl, H.; Stöhr, M.; Jung, T. A.; Gade, L. H. Covalent Assembly of a Two-Dimensional Molecular "Sponge" on a Cu(111) Surface: Confined Electronic Surface States in Open and Closed Pores, *Chem. Commun.* **2014**, *50*, 7628–7631.

114. Gross, L.; Moresco, F.; Savio, L.; Gourdon, A.; Joachim, C.; Rieder, K.-H. Scattering of Surface State Electrons at Large Organic Molecules, *Phys. Rev. Lett.* **2004**, *93*, 2797.

115. Iancu, V.; Deshpande, A.; Hla, S.-W. Manipulation of the Kondo Effect via Two-Dimensional Molecular Assembly, *Phys. Rev. Lett.* **2006**, *97*, 266603.

116. Klappenberger, F.; Kühne, D.; Krenner, W.; Silanes, I.; Arnau, A.; de Abajo, F. J. G.; Klyatskaya, S.; Ruben, M.; Barth, J. V. Tunable Quantum Dot Arrays Formed from Self-Assembled Metal-Organic Networks, *Phys. Rev. Lett.* **2011**, *106*, 026802.

117. Seufert, K.; Auwärter, W.; de Abajo, F. J. G.; Ecija, D.; Vijayaraghavan, S.; Joshi, S.;

Barth, J. V. Controlled Interaction of Surface Quantum-Well Electronic States, *Nano Lett.* **2013**, *13*, 6130–6135.

118. Nicoara, N.; Méndez, J.; Gómez-Rodríguez, J. M. Visualizing the Interface State of PTCDA on Au(111) by Scanning Tunneling Microscopy, *Nanotechnology* **2016**, *27*, 475707.

119. Heller, E. J.; Crommie, M. F.; Lutz, C. P.; Eigler, D. M. Scattering and Absorption of Surface Electron Waves in Quantum Corrals, *Nature* **1994**, *369*, 464–466.

120. Ehm, D.; Hüfner, S.; and Reinert, F.; Kroha, J. ; Wölfle, P.; Stockert, O.; Geibel, C.; Löhneysen, H. v. High-Resolution Photoemission Study on Low-$T_K$ Ce Systems: Kondo Resonance, Crystal Field Structures, and their Temperature Dependence *Phys. Rev. B*, **2007**, *76*, 045117

121. Minamitani, E.; Nakanishi, H.; Diño, W. A.; Kasai, H. Spectroscopic Profiles of a Magnetic Dimer on a Metal Surface, *Solid State Commun.* **2009**, *149*, 1241–1243.

122. Jayaprakash, C.; Krishna-murthy, H. R.; Wilkins, J. W. Two-Impurity Kondo Problem, *Phys. Rev. Lett.* **1981**, *47*, 737–740.

123. Ashcroft, N. W.; Mermin, N. D. *Solid State Physics*, Saunders College, Philadelphia **1976**

124. Li, Q. L.; Zheng, C.; Wang, R.; Miao, B. F.; Cao, R. X.; Sun, L.; Wu, D.; Wu, Y. Z.; Li, S. C.; Wang, B. G.; et al. Role of the Surface State in the Kondo Resonance Width of a Co single Adatom on Ag(111), *Phys. Rev. B* **2018**, *97*, 035417.

125. Limot, L.; Berndt, R. Kondo Effect and Surface-State Electrons, *Appl. Surf. Sci.* **2004**, *237*, 572–576.

126. Moro-Lagares, M.; Fernández, J.; Roura-Bas, P.; Ibarra, M. R.; Aligia, A. A.; Serrate, D. Quantifying the Leading Role of the Surface State in the Kondo Effect of Co/Ag(111), *Phys. Rev. B* **2018**, *97*, 235442.

127. Bao, D.-L.; Zhang, Y.-Y.; Du, S.; Pantelides, S. T.; Gao, H.-J. Barrierless On-Surface Metal Incorporation in Phthalocyanine-Based Molecules, *J. Phys. Chem. C* **2018**, *122*, 6678–6683.

# TOC IMAGE